Laser and Particle Beams (2013), *31*, 635–642.

doi:10.1017/S0263034613000621

Sub-femtosecond hard X-ray radiation generated by electron bunches ejected from water jet

N. ZHAVORONKOV,[1] A. ANDREEV,[1,2] AND K. PLATONOV[2]

[1]Max-Born-Institute, Berlin, German
[2]Vavilov State Instutute, St. Petersburg, Russia

(Received 28 March 2013; Accepted 4 June 2013)

Abstract

A new two-step approach for frequency conversion of laser radiation towards hard X-rays is developed and examined experimentally. Fast electrons are produced in a form of thin jets at the first stage, as an intense femtosecond laser pulses impinges on a micrometer water target. In the second stage the accelerated electrons hit a secondary metal target and generate characteristic K-shell radiation with a duration down to sub-femtosecond. It is shown that counter propagating laser radiation experiences very strong up-shift with up to 6×10^3 times of fundamental frequency by reflection from the electron jets.

Keywords: Electron acceleration; Femtosecond pulses; X-ray

INTRODUCTION

X-ray diffraction and absorption are highly sensitive methods to probe a material structure at the microscopic level with the aim to understand key problems of structure-function relationships. The utilization of ultrafast X-rays allows the probing of structural dynamics for a broad range of systems directly and in real-time. The X-ray pulse duration, as a crucial parameter for effective exploitation of time-resolved methods, demands continuous development of new techniques approaches delivering shorter and shorter pulses. The recent advent of ultrafast, ultra-intense X-rays from free-electron lasers (FEL) gives an outlook to revolutionize research in many branches of science by promising to supply X-ray pulses with duration of less than 10 fs at any desired wavelength in the range of 1.2–22 Å(10–0.5 keV photon energy) (Emma *et al.*, 2010). But because of the very limited number of such facilities, a pressure on beam-time is likely to be considerable. Another essential obstacle for use of X-rays from the free-electron lasers in pump-and-probe methods is the internal jitter that limits the achieved synchronization of the beams to about 140 fs (Dusterer *et al.*, 2011). On the other hand, laser-driven hard X-ray sources offer a comparatively inexpensive, flexible and widely available alternative for studies of transient phenomena of chemical and physical interest by X-ray diffraction or X-ray absorption for tasks with no needs for very high X-ray intensities (von der Linde *et al.*, 2001; Berglund *et al.*, 1998). Recently, reliable and stable X-ray sources based on kilohertz lasers, with the favorable possibility to operate in jitter-free setup (Zhavoronkov *et al.*, 2005), have been reported and are becoming the state of the art equipment for diffraction experiments (Bargheer *et al.*, 2004). Here, we report a new approach for the generation of hard X-rays with durations down to sub-femtosecond in two stages by exploiting femtosecond laser radiation-matter interaction at sub-relativistic and relativistic intensities. In the first stage, hot electrons are produced in a primary water target and accelerated in the forward direction toward the second interaction stage to generate hard X-ray or up-shifted radiation. The energy and duration of the generated characteristic K-shell flashes could be tuned by changing the material and thickness of the secondary target.

Address correspondence and reprint requests to: N. Zhavoronkov, Max-Born-Institute, Max-Born-Str. 2A, 12489 Berlin, German. E-mail: zhavoron@mbi-berlin-de

EXPERIMENTAL SETUP

The experiments were conducted with a use of setup consisting of a Ti:sapphire based laser system, target in a form of cylindrical water jet and equipment for detection and characterization of generated X-rays as it is presented in Figure 1.

The laser system employs chirped pulse amplification (CPA) and consists of a prism-free mode-locked Ti:sapphire oscillator, a regenerative amplifier, and a double-pass booster amplifier, custom designed in a 20 mm long Ti:sapphire rod

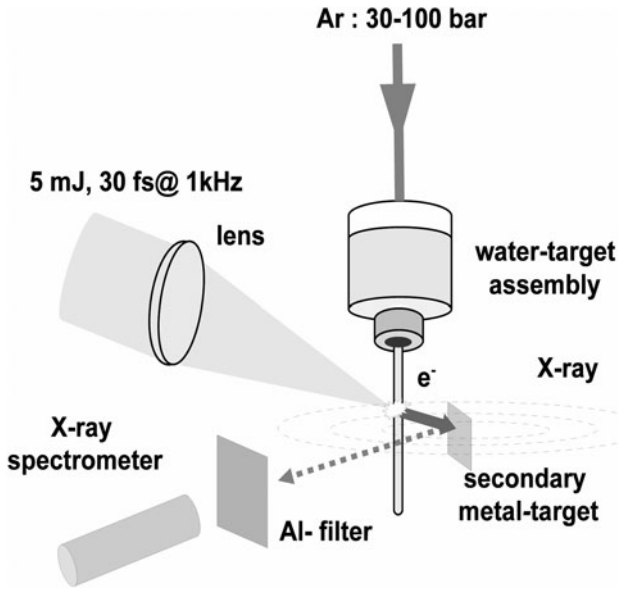

Fig. 1. Experimental set-up of water jet for generation of X-rays from Cu foil as the secondary target.

cooled down to 213 K and placed in a small evacuated chamber. The laser system operates at 1 kHz repetition rate and provides 30-fs pulses at a center wavelength of 795 nm with a maximum pulse energy up to 5 mJ. The long scale temporal structure of the pulses was evaluated by a third order autocorrelator with a dynamic range of eight orders of magnitude. The contrast of the main pulse to amplified spontaneous emission (ASE) was measured to be 10^7. The energy contrast of the main pulse to intrinsic laser system pre-pulse located at 6.5 ps before the main pulse was measured to be as high as 10^5. The laser beam quality analyzed with a Shack-Hartmann wavefront sensor showed a Strehl ratio of 0.973 (RMS = 0.025 waves). The pulse-to-pulse energy fluctuation was measured to be 0.3% (RMS). A focal spot image obtained in the target equivalent plane was monitored by a high magnification imaging system coupled with a CCD detector. The laser focus had a diameter of 6 μm at full width half maximum (FWHM), giving a peak intensity on the beam axis up to 5×10^{17} W/cm^2.

The water jet constructed similar to described elsewhere (Faubel & Kisters, 1989; Tompkins *et al.*, 1998) was formed by forcing a distillate water through the 20 μm circular sapphire orifice (Bird precision Inc.) with 30–100 bar of Ar. Water jet was located vertically in a vacuum chamber which was evacuated down to 10^{-2} mbar. To investigate stability of jet spatial location, we image the jet with the magnification optical system used for laser focusing analysis. A part of laser pulse from Q-switched frequency doubled Nd:YLF laser (523 nm, 200 ns) optically pumping of Ti:sapphire rod in booster amplifier was sent through the system. The magnified jet shadow outside the vacuum chamber demonstrate stable spatial position of the jet within the accuracy of measurement of 1 μm. The *p*-polarized beam from a Ti-sapphire laser system was focused onto the jet at a distance of about 2 mm from the nozzle output, i.e., within the laminar part of the jet, where the cross-section of the jet is well circular.

Emission emanating from the interaction area was studied in a range of 0.5–30 keV with X-ray spectrometer (XR-100CR Amptek Inc.) based on an energy-dispersive Si-photodiode with a resolution of 250 eV. The detector was equipped with lead apertures and 50 μ*m* Al-filter to ensure the operation in single-photon counting mode with a detection solid angle of 0.5 mrad. The spectrometer can be positioned at seven different positions set at 45 degree apart around the target.

X-RAY SPECTRAL PROPERTIES

For laser pulse intensities higher than 10^{16} W/cm^2, supra-thermal electrons are produced primarily by the processes of resonance absorption and vacuum heating. These electrons propagate inside the primary water target, as well as in vacuum along the target surface (Mangles *et al.*, 2006). Most of the electrons moving in vacuum are picked up by laser radiation near the jet surface and accelerated in the forward direction due to radiation pressure effect (Gibbon, 2005; Bulanov *et al.*, 2003; Uhlig *et al.*, 2011). These electrons leave the dense plasma region and penetrate into the material of the second target, producing a burst of incoherent X-rays, composed of continuum bremsstrahlung emission and discrete characteristic X-ray lines. High-energy electrons can create a vacancy by removal (knocking out) one of the inner shells electrons. This vacancy is filled on a femtosecond time-scale by an electron of this ion from a higher energetic level. Since the energy differences between orbitals depends on *Z*, different elements emit X-ray photons with their characteristic wavelength. The radiation was named after the shell to which the electron relaxation takes place. The most energetic photons are radiated by filling the vacancies in the innermost K-shell with photon energies lying in region of hard X-rays. This characteristic radiation has a specific fluorescence feature in a form of isotropic spatial emission.

X-ray photons were detected through collimating apertures at 45 degrees relative to the axis of the laser beam at four different positions oriented at 90 degree relative to each other. The spectra recorded from the different directions show very similar features as well as similar count rates, confirming isotropic spatial distribution of K-shell radiation. The typical recorded X-ray spectrum shown in Figure 2 consist of a broad bremsstrahlung continuum and few lines corresponding to the different K-shell lines been subject of interest. In the spectrum the characteristic lines for Fe ($E_{K_{\alpha 1;2}}$ = 6404 eV; 6390 eV) and Cr ($E_{K_{\alpha 1;2}}$ = 5415 eV; 5406 eV) are well identified. Additional Cu lines at $E_{K_{\alpha 1;2}}$ = eV; 8028 eV, and E_{K_β} = 8905 eV appear in the spectrum only when a secondary target of 50 μm thick Cu foil was placed at a distance of 1 cm from the jet. The Fe - and Cr - lines originate from the orifice holder manufactured from stainless steel with significant portion of Cr, as the accelerated

https://doi.org/10.1017/S0263034613000621 Published online by Cambridge University Press

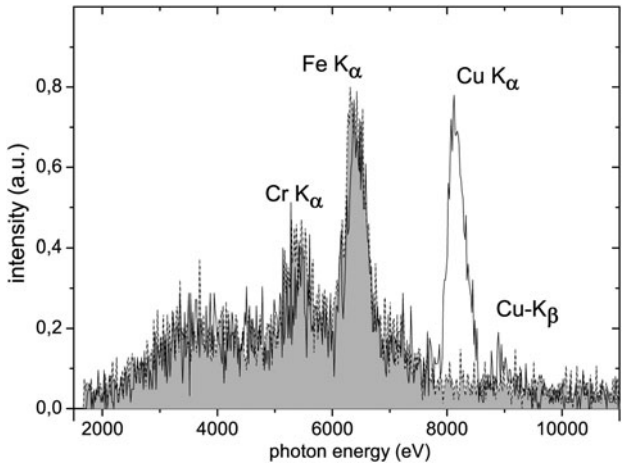

Fig. 2. X-ray spectra obtained from only water jet (filled curve) and with Cu foil as the secondary target.

electrons hit this holder, located only 2 mm above the water-jet-laser interaction point and extended till the location of the secondary Cu target. We define an angle of incidence as the angle between the laser-beam axis and normal to the target surface at the point where the laser-beam hits the target. The K_α yield depends strongly on angle of incidence. We can detect only few photons at frontal incidence (0 degree) and reach a maximum around 45 ± 10 degrees. The K_α photon flux was calculated from the spectra detected by Amptek spectrometer, calibrated by use of a ^{55}Fe radionuclide source for absolute numbers of photons. Isotropic emission in 4π was assumed for the calculation of the X-ray yield from the spectrum. Our measurements give values of the total and the Cu-K_α X-ray fluxes of up to 1.3×10^6 and 3.5×10^5 photons/pulse respectively. One way to increase the useful X-ray photon flux could be a radical increase of the repetition rate for a driving laser radiation up to few tens of kHz. This can easily be achieved for jet-targets with typical flow velocities of 10 to 100 m/s, which will allow repetition rates as higher as 100 kHz. In a conventional laser-assisted X-rays generation with solid metal targets formed as rotating disks, tapes or wires such repetition rates are not achievable, because of too low velocity of transportation. On the other hand, liquid metal jet (Zhavoronkov *et al.*, 2004) targets eject copious amounts of target material toward the focusing optics, demanding special protection to prevent contamination or/and permanent damage. Our design with a secondary target has the great advantage of completely contamination-free, with no metal debris, because there is no interaction of the laser beam with the material of metal target.

ANALYSIS OF THE EXPERIMENTAL RESULTS AT SUB-RELATIVISTIC LASER INTENSITY

Now we will estimate a possibility and necessary experimental conditions for generation of 10^6 X-ray photons from the secondary target. To do this we have to determine the number of fast electrons produced by laser pulse in water target and after that to find the number of X-rays photons with a use of cross-section for generation of K-shell photon by scattering of the fast electron. With help of one-dimensional quasi-stationary model developed in Nakano *et al.* (2004), where the interaction of fast electrons with solid foil of thickness d is considered, we can estimate the number of K_α photons generated by fast electrons of number N_{eh} into solid angle Ω as follows:

$$N_{ph} = N_{eh}\frac{\Omega}{4\pi}5,7\cdot 10^{-4}\left(\frac{Z*^2}{1+10^{-2}Z*^4}\right)\kappa^{0.67} \times exp(-\kappa)\left[1-exp\left(-\frac{d_\mu}{2Z*^2}\right)\right], \quad (1)$$

where

$$\kappa = Z*^{1-0.25}\frac{0.97}{(\eta I_{16})^{2/3}},\ Z* = \frac{Z_n}{13},\ d_\mu = d/1\mu m,\ I_{16} = I_l/10^{16}\ \mathrm{W/cm^2}.$$

Taking for the water target $Z_n = 8$, where Z_n is the nuclei charge, and $d = 20\ \mu m$, and from the experimental conditions $k \approx 1$ at $I_{16} \approx 50$ with $N_{ph} = 3.5 \times 10^5$ we arrive at the result $N_{eh} \approx 10^{10}$. Since the laser prepulse before the main pulse creates a plasma corona of micron length ΔR, we can identify resonant absorption as the main channel for absorption of the laser radiation. The intensity of a Gaussian laser beam with its axis shifted on the distance $\rho = R \sin\alpha$ from the target center, where R is the jet radius and $\alpha \in [0;\pi/2]$ is the angle of incidence, is $I(\alpha) = \pi^{-1/2} I_0 exp(-(R \sin\alpha - \rho)^2/r_l^2)$, with r_l as a radius of the laser beam. According to the theory for resonant absorption developed in (Andreev *et al.*, 1983) the absorption coefficient is determined as follows:

$$\eta = \frac{1}{\sqrt{\pi}}\sum_{l=0}^{\infty} f_{lr}\int_0^1 P_l(x)exp\left[-\frac{(R\sqrt{1-x^2}-\rho)^2}{r_l^2}\right]dx, \quad (2)$$

where $P_l(x)$ is the Legandre polynomial and f_{lr} is the resonant absorption coefficient defined as:

$$f_{lr} = \begin{cases} 2(k\Delta R)^{2/3}l^2/k^2R^2 & \text{if } l < 0.6kR/(k\Delta R)^{1/3} \\ 0.5 & \text{if } 0.6kR/(k\Delta R)^{1/3} < l < 0.8kR/(k\Delta R)^{1/3} \\ 2\exp(-4k\Delta Rl^3/3k^3R^3) & \text{if } 0.8kR/(k\Delta R)^{1/3} < l \end{cases}.$$

The absorption coefficient calculated from Eq. (2) for frontal incidence of the laser beam on the water jet with $r_l = 5\ \mu m$, $\rho = 0$, $R = 10\ \mu m$ and $\Delta R = 1\ \mu m$ is $\eta = 0.1$. This value is small because of non-optimal angle of incidence. We can estimate the average electron energy as $T_e \sim (\eta\varepsilon_l/N_e) \leq 500$ eV for total number of $N_e \approx 10^{14}$ electrons from the O^{+3} and H^+ ions in the volume-fragment of water irradiated by the laser beam with a pulse energy of $\varepsilon_l = 5$ mJ. Taking into account a Maxwellian distribution for the electron energy, the number

https://doi.org/10.1017/S0263034613000621 Published online by Cambridge University Press

of electrons with $T_e \geq 10$ keV will be much less than 10^{10}. Thus the necessary amount of hot electrons cannot be produced from the target volume homogenously heated by the laser pulse, instead it should be generated through resonant absorption from a surface area of the water cylinder directly irradiated by the laser pulse. For such scenario the amount of hot electrons could reach a value of 5×10^{10}. The propagation length for a thermal wave l_T (τ) at the time $\tau \approx 2R/v_e$, where v_e is velocity of the hot electrons, obtained from hydro-dynamical simulation, is only 2 μm. Taking into account the free path of hot electrons in the 20 μm cold water jet and a Coulomb barrier at the back side of the target $E_c = e^2 N_{eh}^2/2R$, only electrons with an energy higher than 50 keV are able to reach the secondary target and contribute to X-ray generation. The number of such electrons for frontal incidence is pretty low. For larger angles of incidence, interplay between the involved phenomena leads to conditions favorable for X-rays generation. First, resonant absorption is more efficient with growing absorption coefficient up to $\eta = 0.2$ for angle of incidence of about 40 degrees ($\rho = 8\ \mu m$). Second, the path of the electrons inside the cold target (from the point of generation to the back side of the target) decreases, reducing the dissipation of electron energy. Third, the electrons escape more efficiently towards vacuum from the plasma region because of the reduction of Coulomb barrier by component of the laser field normal to the target surface. To describe more accurately the process of electron generation and prove the experimental data, we performed simulations for the interaction of the laser pulse with water cylinder by two-dimensional (2D) particle in cell (PIC) code (Kemp & Ruhl 2005). The laser pulse parameters were taken from the experiment. A water cylinder with 20 μm diameter and wall thickness of 1 μm was used as a target. It consisted of protons and O^{+3} ions in a ratio of densities 2:1. The absence of bulk water did not change perceptibly the amount of generated fast electrons, but enhances the simulation accuracy. The simulations were performed within a box of 100 $\mu m \times 100\ \mu m$. The time onset is taken as the moment when the laser pulse enters the simulation box, thus, the maximum of the laser pulse reaches the target surface at $t_m = 137$ fs. Boundary conditions in the simulation box were periodical for the particles and "outgoing" for fields. To extrapolate the data from 2D simulations towards the three-dimensional case, we integrate the calculated particle number across the beam cross-section along the target cylinder. The results of the numerical simulation show that most of fast electrons are directed inside the target towards its center, whereas another type are emitted from the plasma region into vacuum in the form of jets (e-jets) at a tangent to the target surface, as it is evident from Figure 3a (insert). Only electrons with an energy of ≥ 10 keV, and directed toward the secondary target within the angle of 0.35 rad, are able to reach the target and contribute to K_α generation. It follows from the phase diagram $p_z - y$ for such electrons in Figure 3b that they are localized at the surface of the water target at $t_m = 137$ fs, when the maximum of laser pulse reaches the target. The path of these electrons within the water jet is small as comparable to the whole water cylinder diameter and their outcome from the jet is facilitated by diffracted component of laser field as it is could be noticed in Figure 3. The total number of the electrons N_{eh} in Figure 3b is $\approx 5 \times 10^{10}$. The density of hot electrons at time $t = 210$ fs after passing through the target and emerging into vacuum is depicted in Figure 3a in red, whereas the blue dots present the electron distribution at $t_m = 137$ fs. Only about of 5% of the initial N_{eh} electrons are directly ejected into vacuum in the form of e-jets. The rest of the electrons have to pass through the water before appearing in vacuum on the another side of the water jet. The total number of the electrons that can be ejected into vacuum is $\approx 10^{10}$, correlating well with the number estimated above. At the used in the experiment laser intensity of 5×10^{17} W/cm^2 the generated electrons demonstrate quasi-homogenous spatial density profile without any remarkable density modulation as it is shown in Figure 3b. This electron bunch has duration equal to duration of the laser pulse. The characteristic K_α photons, arising from

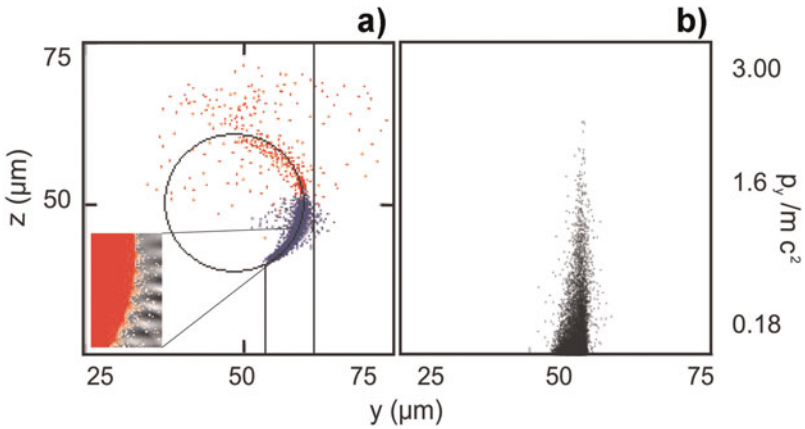

Fig. 3. (Color online) Results of 2D PIC simulations: (**a**) hot electron density at 137 fs (blue) and 210 fs (red). Two vertical lines mark the laser beam position, (**b**) phase diagram $p_z - y$ for the electrons with energy ≥8keV.

https://doi.org/10.1017/S0263034613000621 Published online by Cambridge University Press

interaction of electrons with the secondary target, will radiate out of target only if they are generated within the K_α's attenuation length of about 30 μm (http://henke.lbl.gov). Hence, duration of the generated K_α flash will exceed the duration of the electron bunch by the time necessary electrons to pass the 30 μm of Cu, that, according to calculation with code Casino, is about 120 fs. Hereby, duration of the generated X-rays is estimated to be as long as 150 fs. Since spectrum of the electron bunch shows exponential decay towards high energies, the X-ray pulse will have similar temporal profile with exponentially extended tail.

THEORETICAL APPROACH FOR RELATIVISTIC LASER INTENSITY

Our simulations similar to the presented above, but performed at different laser intensity shown that the total number of fast electrons as well as the number of them coming out in vacuum increases proportionally to the laser intensity, and is only a weakly dependent on the scale of the plasma corona at high laser intensity. To get deeper insight the process as well as to find a way to drastically increase the number of generated fast electrons, we perform a simulation for a laser intensity as high as 10^{20} W/cm^2 with 20 fs pulses and square water target of density 4×10^{22} cm^{-3}. The square geometry is chosen to increase the interaction length of the laser field with electrons. At ultrarelativistic intensity most of the ejected fast electrons are transferred into vacuum and accelerated in the forward direction as a bunch, named above e-jet (Naumova *et al.*, 2004). In Figure 4a (inset) these e-jets are depicted in red. The distortion of the laser wavefront on the side surfaces of the rectangular target (Fig. 4a insert) could be explained by diffraction on the laser field on the left and right corners of the target. These corners show themselves as sources of secondary cylindrical waves. The theory of wave diffraction on rectangular conductive wedge (Landau & Lifshic, 1960) describes the field close to corner as:

$$E_y(x,y) = E_0\frac{-2\sqrt{2}}{\sqrt{3\pi kr}}exp(i(kr+\pi/4))\Big[\frac{1}{1+2\cos(2\phi/3-2\pi/3)} + \frac{1}{1+2\cos(2\phi/3)}\Big], \quad (3)$$

where $\phi \in [0, \pi]$, $1+2\cos(2\phi/3-2\pi/3) > 2/\sqrt{kr}$, $1+2\cos(2\phi/3) > 2/\sqrt{kr}$, r—distance from the corner, ϕ-angle to axis z, $k=\omega_l/c$, E_0—incident laser field. Eq. (3) describes divergent cylindrical wave with the amplitude reaching maxima at the angles ϕ closed to 0 or π, as it could be seen in Figure 4a insert. The Eq. (3) is valid for $kr=\omega_l/c \in [2; 20]$. Eq. (3) presents a linear solution and can not describe formation of short wavelength radiation visible in Figure 4a (insert) in a form of thin drey lines collinear to electron jets. This effect results from nonlinear interaction and from oscillation of reflecting target surface under influence of high intensity laser field. It was recently shown (Naumova *et al.*, 2004; Liseikina *et al.*, 2010; Gonoskov *et al.*, 2011; Lavocat-Dubuis *et al.*, 2011), that for relativistic intensities the reflected from the target radiation contains short wavelength radiation with durations in attosecond range. For taken conditions the thickness of the e-jet is $d_{e-jet} \approx 20$ nm with a duration of $\approx 70as$ $(1as = 10^{-18}\ s)$ and density $\sim 4\times10^{21}\ cm^{-3}$. Thus for a laser beam with a diameter of $6\mu m$ we obtained about 5×10^8 electrons with energy of ≈ 25 MeV in a jet. The number of extracted electrons can be estimated analytically as $N_e \approx n_e\ l_{extr}S$, where $l_{extr} = E_0/en_e = 2\lambda n_c\sqrt{1.37I_{18}}/n_e$, n_e is electron density in the target, $I_{18} = I_l/10^{18}$, n_c is the critical plasma density, and S is the surface area of interaction. For these parameters we obtain $N_e \approx 10^9$, very close to the value from the numerical simulations. The characteristic size of the electron orbit along electric field can be estimated as (Gibbon 2005) $r_{eh} = eE_0/m_e\omega^2 = \lambda_l\ a/2\pi \approx 1.2\,\mu m$, for $a = 10$, that is the height of the e-jets from Figure 4a. The

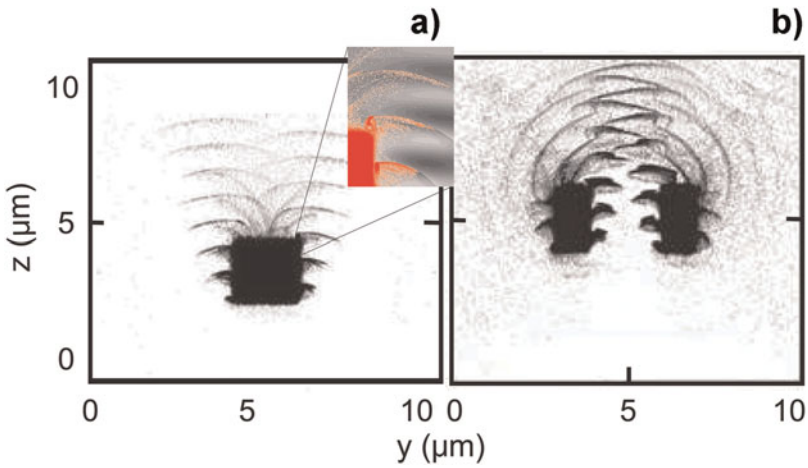

Fig. 4. (Color online) Electron density distribution for (**a**) square target, and (**b**) for square target with hole. In the magnified fragment the electrons are denoted by red and electric field by gray colors.

https://doi.org/10.1017/S0263034613000621 Published online by Cambridge University Press

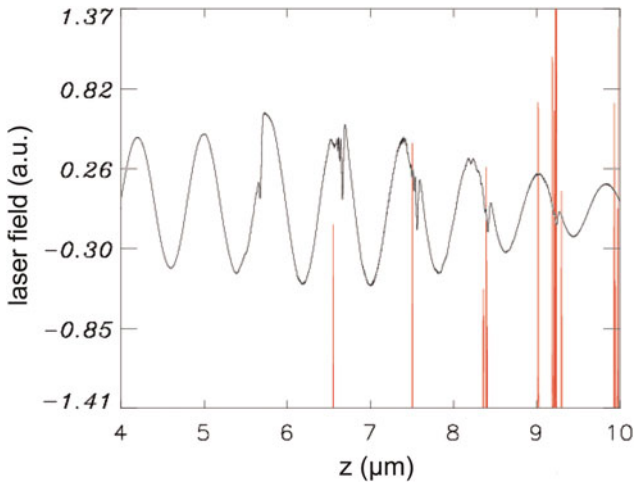

Fig. 5. (Color online) Snap-shot of the laser field (grey line) and the electron jets (red lines) as they co-propagate along z-axis towards the secondary target.

resulting electron flux is composed of a train of jets from the single electron jets created by each laser wave period. The jets will propagate a distance $L \sim ct_l\,(\varepsilon_{eh}/m_e c^2)$ and be accelerated further by the laser field. Figure 5 presents a snapshot of the laser field — electron jets composition along axis z. However, when the laser wave overtakes the bunch it will begin to expand in time as a result of influence of Coulomb forces. Very short X-ray flashes will be generated from a secondary target positioned at the distance L. We simulated the process of interaction by PIC code with extended simulation box size of 300 micrometers to cover the distance L. The results demonstrate, that the thickness of e-jets are in quasi-steady state under stabilizing action from co-propagating diffracted laser wave, as it is well demonstrated in Figure 5, with the thickness of single jet within 20–40 nm. The calculated electron distribution functions have a width of 8–10 MeV, that will not contribute to pronounced extension of K_α pulse duration at given distance L. The optimal secondary target should be constructed from high-Z materials like Ag, for which the conversion efficiency of electron energy in K_α photons is defined as $\eta_k = n_a \sigma_z l_{in}$, where $\sigma_z \approx \sigma_0 \ln(\epsilon_{eh}/0.1\ \mathrm{MeV})$ (Andreev & Platonov, 2011), $\sigma_0 = 5barn$, n_a is concentration of Ag-atoms, $l_{in} \approx 20\ \mu m$—the free path of K_α quantum in solid Ag. The total number of generated K_α photons for a single electron bunch is ~10^6. The duration of the generated flash can be estimated as ~l_{in}/c, i.e., longer than the laser period. Thus, K_α flashes generated from the different single electron bunches will merge into one long X-ray pulse of up to 100 fs duration. To resolve the X-ray pulses produced by a single electron jet, the thickness of the secondary target l_t should be in the range of $d_{jet} \le l_t \le \lambda$, resulting in choice between higher conversion efficiency or shorter pulse duration. For example, the duration of K_α pulses generated in a 200 nm Ag target, comprising a film-target on a polymer substrate to avoid recirculation of electrons (Mackinnon *et al.*, 2002), would be $\tau_x \le 0.7$ fs. The conversion efficiency for the considered parameters is 10^{-4}, that together with the $N_{eh} \approx 10^9$ obtained in simulation gives the number of generated K_α photons as high as $N_{ph} \approx 10^5$ with the corresponding spectral brightness $B \approx 3 \times 10^9$ $phot/mm^2\ sr$ for single jet. Generation of a single X-ray pulse instead of pulse train could be achieved through the use of few-cycle laser pulses. It should be emphasized that in our approach the electrons are originated in a form of jets directly from the water surface with the period of laser field and propagate further accompanied by laser field under action of pondermotive force preventing a temporal spreading of the jets. The process differentiates from phenomena in another approaches (Giulietti *et al.*, 2008; Glinec *et al.*, 2005), where the MeV electron bunches are formed by wake-field acceleration in plasma and have the period of plasma waves.

RELATIVISTIC FREQUENCY MULTIPLICATION

The generated e-jets provide a possibility for improvement of one interesting application — relativistic frequency multiplication, where the frequency of laser field is multiplied by a factor of $4\gamma^2$ when reflects from high density plasma slab accelerated by ultraintense laser field in radiation pressure dominant regime (Bulanov *et al.*, 2003; Kando *et al.*, 2007; Esirkepov *et al.*, 2009). Under the Fresnel approximation, and for laser intensities below 10^{18} W/cm^2 necessary to avoid relativistic transparency, we estimate the reflection coefficient from the periodical e-jet structure as:

$$R = R_l \frac{\sin^2(2NL_b\omega\gamma_b^2/c)}{\sin^2(2L_b\omega\gamma_b^2/c)},\ R_l = \left(\frac{2\pi e^2 n_{eb} l_b}{m_e \omega c}\right)^2, \qquad (4)$$

where n_{eb}—electron density in the e-jet, l_b- jet thickness, L_b—distance between the e-jets, N—the total number of the generated e-jets. For single e-jet taken from Figure 4 with thickness of $l_b \sim 20$–50 nm, $n_b = 4 \times 10^{21}$ cm^{-3} and at $\omega \sim \omega_l$ the reflection coefficient reaches $R_l \approx 4 \times 10^{-5}$. When employing a sectioned water target the single e-jet is produced twice for each period of the laser field, as shown in Figure 4b. Since the spatial separation $L_b = \lambda/2$ between the jets can be taken as a constant for the time of interaction with the incident light, the entire e-jets ensemble forms a spatially electron density with perfect period. Figure 5 shows such periodic electron structure only with twice smaller period for solid target from Figure 4a. For 20 fs laser pulses the number of generated jets N will be around 15. Multiple reflection from successive e-jets is coherent and could be constructive if $\lambda_l = n\pi/\gamma_b\ w^*$, where n is integer. Under this condition the back-reflections will experience a drastic enhancement and will reach the resonance value of $R \approx (N)^2 R_l$, that would be as high as 0.1%. From the other hand, because of large value of arguments for sin-functions in Eq. (4), e.g., for

https://doi.org/10.1017/S0263034613000621 Published online by Cambridge University Press

20 MeV electrons $\gamma_b \cong 40$ and $2\gamma^2 = 3.2 \times 10^3$, even a small spread of γ_b will cause a large changing in the arguments value. As a consequence, the resonant reflection can be suppressed when Eg. (4) have to be averaged within even 10% spread around a mean γ_b value. For such case the resultant reflection coefficient will be reduced toward the trivial composition of the single components in a form $R \approx N\ R_l$. By reflection on the formed e-jets with 20 MeV electrons and $\lambda_l = 800$ nm the up-shifted frequency can reach the value up to 6×10^3 of ω_l corresponding $\lambda_r \approx 1.3\dot{A}$ and photon energy of $\hbar w \approx 10$ keV, that is the energy range for Cu K-shell radiation. We estimate the reflected radiation brightness of $B \approx 3 \times 10^{21}\ phot/mm^2\ sr$. It is worth to note, that the resonance conditions could be satisfied for another wavelength by carrying out the scattering at the angle of θ_l from $\lambda_l cos\theta_l = n\pi/\gamma w^*$ giving possibility to tune the wavelength of up-converted radiation applying f.i. radiation from tunable laser at different angles of incidence. Additional advantage of the presented relativistic frequency multiplication method with a use of sectional target by comparison to the standard "one step" or the new "two-step" approaches for generation of K – lines is well defined angular directionality. Moreover, the composition of the e-jets located after the water target as it is shown in Figure 4a exhibit the specific funnel form, that will act as focusing element for converted radiation if the original ω_l wave hits the e-jet structure from above.

The generated by frequency multiplication X-rays will reflect the electron energy spread within the e-jets in terms of photon energy spectrum. Additionally to the spectral spread, the reflected radiation could be also chirped due to acceleration of e-jets. From another side the large possible spectral spread of reflected photon is favored for generation of shortest pulses. The calculations performed in this work for plane e-jets demonstrate the upper limit for efficiency and frequency conversion. Further examination of relativistic frequency multiplication on e-jets including pulse duration, spectral bandwidth, spectral chirp and brightness of the source is out of the main scope of this paper and will be discussed in future publications.

CONCLUSION

We propose the new approaches for the generation of hard X-rays and for the increasing efficiency of frequency up-conversion on the basis of the interaction of jets of electrons created out of micrometer-sized water targets with a secondary metal target or with a counter-propagating laser radiation. A proof-of-principle experiment to generate $Cu\ K_\alpha$ photons at sub-relativistic laser intensity supports the numerical simulation and demonstrates good perspectives for the new type of tunable sub-femtosecond laser-driven X-ray source with the advantage of operation in debris-free mode. A. A. A. and K. P. acknowledge the provided computation resources of JSC at project HBUIS, and support from RFBR (project 09-02-12129-OFI.M)

REFERENCES

Andreev, A., Kryzhanovskiy, N. & Solovyev, N. (1983). Absorption and scattering of laser beam in spherical plasma target. *Opt. Spectrosc.* **54**, 547–566.

Andreev, A. & Platonov, K. Yu. (2011). Hybrid model of ion acceleration in laser plasma of flat heterogeneous target. *Opt. Spectrosc.* **101**, 23–29.

Bargheer, M. Zhavoronkov, M., Gritsai, Y, Woo, J.C., Kim, D.S., Woerner, M. & Elsaesser, T. (2004). Coherent atomic motions in a nanostructure studied by femtosecond X-ray diffraction. *Sci.* **361**, 1771–1773.

Berglund, M., Rymell, L., Hertz, H.M. & Wilheim, T. (1998). Cryogenic liquid-jet target for debris-free laser-plasma soft X-ray generation. *Rev. Sci. Instrum.* **69**, 2361–2364.

Bulanov, S.V., Esirkepov, T. & Tajima, T. (2003). Light intensification towards the Schwinger limit. *Phys. Rev. Lett.* **91**, 085001–4.

Dusterer, S., Radcliffe, P., Bostedt, C., Bozek, J., Cavalieri, A.L., Coffee, R., Costello, J.T., Cubaynes, D., DiMauro, L.F., Ding, Y., Doumy, G., Grüner, F., Helml, W., Schweinberger, W., Kienberger, R., Maier, A.R., Messerschmidt, M., Richardson, V., Roedig, C., Tschentscher, T. & Meyer, M. (2011). Femtosecond x-ray pulse length characterization at the Linac Coherent Light Source free-electron laser. *New J. of Physics* **13**, 093024–10.

Emma, P. Akre, R., Arthur, J., Bionta, R., Bostedt, C., Bozek, J., Brachmann, A., Bucksbaum, P., Coffee, R., Decker, F.-J., Ding, Y., Dowell, D., Edstrom, S., Fisher, A., Frisch, J., Gilevich, S., Hastings, J., Hays, G., Hering, Ph., Huang, Z., Iverson, R., Loos, H., Messerschmidt, M., Miahnahri, A., Moeller, S., Nuhn, H.-D., Pile, G., Ratner, D., Rzepiela, J., Schultz, D., Smith, T., Stefan, P., Tompkins, H., Turner, J., Welch, J., White, W., Wu, J., Yocky, G. & Galayda, J. (2010). First lasing and operation of an ångstrom-wavelength free-electron laser. *Nat. Photon.* **4**, 641–647.

Esirkepov, T., Bulanov, S.V., Kando, M., Pirozhkov, A.S. & Zhidkov, A.G. (2009). Boosted high-harmonics pulse from a double-sided relativistic mirror. *Phys. Rev. Lett.* **103**, 025002–4.

Faubel, M. & Kiters, Th. (1989). Non-equilibrium molecular evaporation of carboxylic acid dimers. *Nat.* **339**, 527–529.

Gibbon, P. (2005). *Short Pulse Laser Interaction with Matter*. London: Imperial College Press.

Gonoskov, A., Korzhimanov, A.V., Kim, A.V., Marklund, M. & Sergeev, A.M. (2011). Ultrarelativistic nanoplasmonics as a route towards extreme-intensity attosecond pulses. *Phys. Rev. E* **84**, 046403–7.

Giulietti, A., Bourgeois, N., Ceccotti, T., Davoine, X., Dobosz, S., DâOliveira, P., Galimberti, M., Galy, J., Gamucci, A., Giulietti, D., Gizzi, L.A., Hamilton, D.J., Lefebvre, E., Labate, L., Marquès, J.R., Monot, P., Popescu, H., Réau, F., Sarri, G., Tomassini, P. & Martin, P. (2008). Intense γ-ray source in the giant-dipole-resonance range driven by 10-TW laser pulses. *Phys. Rev. Lett.* **101**, 105002–4.

Glinec, Y., Faure, J., Pukhoc, A., Kiselev, S., Gordienko, S., Mercier, B. & Malka, V. (2005). Generation of quasi-monoenergetic electron beams using ultrashort and ultraintense laser pulses. *Laser Part. Beams* **23**, 161–166.

Kando, M., Fukuda, Y., Pirozhkov, A.S., Ma, J., Daito, I., Chen, L.-M., Esirkepov, T. Zh., Ogura, K., Homma, T., Hayashi, Y., Kotaki, H., Sagisaka, A., Mori, M., Koga, J.K., Daido, H.,

https://doi.org/10.1017/S0263034613000621 Published online by Cambridge University Press

Bulanov, S.V., Kimura, T., Kato, Y. & Tajima, T. (2007). Demonstration of laser-frequency upshift by electron-density modulations in a plasma wakefield. *Phys. Rev. Lett.* **99**, 135001–4.

Kemp, A.J. & Ruhl, H. (2005). Multispecies ion acceleration off laser-irradiated water droplets. *Phys. of Plasmas* **12**, 033105–10.

Lavocat-Dubuis, X. Vidal, F., Matte, J-P., Kieffer, J-C. & Ozaki, T. (2011). Multiple attosecond pulse generation in relativistically laser-driven overdense plasmas. *N J. Phys.* **13**, 023039–12.

Liseikina, S., Pirner, S. & Bauer, D. (2010). Relativistic attosecond electron bunches from laser-illuminated droplets. *Phys. Rev. Lett.* **104**, 095002–4.

Mangles, S.P.D., Walton, B.R., Najmudin, Z., Dangor, A.E., Krushelnick, K., Malka, V., Manclossi, M., Lopes, N., Carias, C., Mendes, G. & Dorchies, F. (2006). Table-top laser-plasma acceleration as an electron radiography source. *Laser Part. Beams* **24**, 185–190.

Nakano, H., Andreev, A. & Limpouch, J. (2004). Femtosecond X-ray line emission from multilayer targets irradiated by short laser pulses. *Appl. Phys. B* **79**, 469–476.

Naumova, N., Sokolov, I., Nee, J.s, Maksimchuk, A., Yanovsky, V. & Mourou, G. (2004). Attosecond electron bunches. *Phys. Rev. Lett.* **93**, 195003–4.

Landau, L.D. & Lifshitz, E.M. (1960). *Electrodynamics of continuous Media*. New York: Pergamon Press.

Mackinnon, A., Sentoku, Y., Patel, P.K., Price, D.W., Hatchett, S., Key, M.H., Andersen, C., Snavely, R. & Freeman, R.R. (2002). Enhancement of proton acceleration by hot-electron recirculation in thin foils irradiated by ultraintense laser pulses. *Phys.Rev. Lett.* **88**, 215006–4.

Tompkins, R.J., Mercer, I.P., Fettweis, M., Barnett, C.J., Klug, D.R., Porter, Lord G., Clark, I., Jackson, S., Matousek, P., Parker, A.W. & Towrie, M. (1998). 5–20 keV laser-induced x-ray generation at 1 kHz from a liquid-jet target. *Rev. Sci. Instrum.* **69**, 3113–3117.

Von der Linde, D., Sokolowski-Tinten, K., Blome, Ch., Dietrich, C., Zhou, P., Tarasevitch, A., Cavalleri, A., Siders, C.W., Barty, C.P.J., Squier, J., Wilson, K.R., Uschmann, I. & Forster, E. (2001). Generation and application of ultrashort X-ray pulses. *Laser Part. Beams* **19**, 15–22.

Uhlig, J., Wahlstrom, C.-G., Walczak, M., Sundstrom, W. & Fullagar, W. (2011). Laser generated 300 keV electron beams from water. *Laser Part. Beams* **29**, 415–424.

Zhavoronkov, N., Gritsai, Y, Bargheer, M., Woerner, M, Elsaesser, T., Zamponi, F., Uschmann, I. & Förster, E. (2005). Microfocus Cu K-alpha source for femtosecond x-ray science. *Opt. Lett.* **30**, 1737–1739.

Zhavoronkov, N., Gritsai, Y., Korn, G. & Elsaesser, T. (2004). Ultra-short efficient laser-driven hard X-ray source operated at a kHz repetition rate. *Appl. Phys. B* **79**, 663–667.

https://doi.org/10.1017/S0263034613000621 Published online by Cambridge University Press